European Congress on Computational Methods
in Applied Sciences and Engineering (ECCOMAS 2012)
J. Eberhardsteiner et.al. (eds.)
Vienna, Austria, September 10-14, 2012

A VOLUME MESH FINITE ELEMENT METHOD FOR PDES ON SURFACES

Maxim A. Olshanskii[1], **Arnold Reusken**[2], **and Xianmin Xu**[2,3]

[1] Department of Mechanics and Mathematics, Moscow State University,
Moscow 119899, Russia
e-mail: Maxim.Olshanskii@mtu-net.ru

[2] Institut für Geometrie und Praktische Mathematik, RWTH-Aachen University
D-52056 Aachen, Germany
e-mail: {reusken,xu}@igpm.rwth-aachen.de

[3] LSEC, Institute of Computational Mathematics and Scientific/Engineering Computing,
NCMIS, AMSS, Chinese Academy of Sciences, Beijing 100190, China

Keywords: surface finite element, surface SUPG stabilization, residual-type surface finite element error indicator

Abstract. *We treat a surface finite element method that is based on the trace of a standard finite element space on a tetrahedral triangulation of an outer domain that contains a stationary 2D surface. This surface FEM is used to discretize partial differential equation on the surface. We demonstrate the performance of this method for stationary and time-dependent diffusion equations. For the stationary case, results of an adaptive method based on a surface residual-type error indicator are presented. Furthermore, for the advection-dominated case a SUPG stabilization is introduced. The topic of finite element stabilization for advection-dominated surface transport equations has not been addressed in the literature so far.*

1 INTRODUCTION

Moving hypersurfaces and interfaces appear in many physical processes, for example in multiphase flows and flows with free surfaces. Certain mathematical models involve elliptic partial differential equations posed *on* such surfaces. This happens, for example, in multiphase fluids if one takes so-called surface active agents (surfactants) into account [10]. In mathematical models surface equations are often coupled with other equations that are formulated in a (fixed) domain which contains the surface. In such a setting, a common approach is to use a splitting scheme that allows to solve at each time step a sequence of simpler (decoupled) equations. Doing so one has to solve numerically at each time step an elliptic type of equation on a surface. The surface may vary from one time step to another and usually only some discrete approximation of the surface is available. A well-known finite element method for solving elliptic equations on surfaces, initiated by the paper [4], consists of approximating the surface by a piecewise polygonal surface and using a finite element space on a triangulation of this discrete surface. This approach has been analyzed and extended in several directions in a series of papers, e.g. [2, 5, 8, 6, 7, 9]. Another approach has recently been introduced in [1]. The method in that paper applies to cases in which the surface is given implicitly by some level set function and the key idea is to solve the partial differential equation on a narrow band around the surface. Unfitted finite element spaces on this narrow band are used for discretization. Yet another method has been studied in [12]. The main idea of the method in the latter paper to use time-*in*dependent finite element spaces that are induced by triangulations of an "outer" domain to discretize the partial differential equation on the surface. The method is particularly suitable for problems in which the surface is given implicitly by a level set or VOF function and in which there is a coupling with a flow problem in a fixed outer domain. If in such problems one uses finite element techniques for the discetization of the flow equations in the outer domain, this setting immediately results in an easy way to implement discretization method for the surface equation. The approach does not require additional surface elements. If the surface varies in time, one has to recompute the surface stiffness matrix using the same data structures each time. Moreover, quadrature routines that are needed for these computations are often available already, since they are needed in other surface related calculations, for example surface tension forces. Opposite to the method in [1] the method from [12] does not use an *extension* of the surface partial differential equation but instead uses a *restriction* of the outer finite element spaces. This method has been further investigated in [11, 3]. In the paper [3] a posteriori error indicators for this surface finite element method are introduced and analyzed.

In this paper, we reconsider this volume mesh finite element method. We review the main ideas and results from [12, 3] and illustrate its behavior by presenting results of numerical experiments for different classes of problems. We restrict ourselves to the case of a *stationary* surface. Stationary and time-dependent diffusion (surface heat diffusion) problems are treated. For the stationary case the error indicator from [3] is briefly recalled and its performance for a surface diffusion problem with a nonsmooth solution is demonstrated. A new aspect, that has not been studied in the literature so far, is a stabilization for advection-dominated problems. We introduce a surface variant of the SUPG stabilization technique and show that this stabilization performs well both for stationary and time-dependent advection-dominated surface transport equations.

2 BASIC IDEA OF THE VOLUME MESH FINITE ELEMENT METHOD

In this section, we explain the basic idea of our finite element method by applying it to a Laplace-Beltrami model problem. Let $\Omega \subset \mathbb{R}^3$ be a bounded polyhedral domain and $\Gamma \subset \Omega$ a closed smooth hyper-surface in $\mathbb{R}^3$. Denote by $\mathbf{n}_\Gamma$ the unit outward normal vector on Γ. For a sufficiently smooth function $g : \Omega \to \mathbb{R}$, its surface gradient on Γ is defined as

$$\nabla_\Gamma g = \nabla g - (\nabla g \cdot \mathbf{n}_\Gamma)\mathbf{n}_\Gamma.$$

This definition is intrinsic for Γ and does not depend on how g is extended outside Γ. The Laplace-Beltrami operator on Γ is given by

$$\Delta_\Gamma g := \nabla_\Gamma \cdot \nabla_\Gamma g.$$

We consider the Laplace-Beltrami equation

$$-\Delta_\Gamma u + c(\mathbf{x})u = f \quad \text{on } \Gamma. \tag{1}$$

Here c and f are given functions, with $c(\mathbf{x}) \geq 0$ on Γ. If c is identically zero on Γ we add the conditions $\int_\Gamma u \, \mathrm{d}\mathbf{s} = \int_\Gamma f \, \mathrm{d}\mathbf{s} = 0$ to ensure well-posedness.

The corresponding variational formulation is as follows: Find $u \in V$ such that

$$\int_\Gamma \nabla_\Gamma u \cdot \nabla_\Gamma v \, \mathrm{d}\mathbf{s} + \int_\Gamma c(\mathbf{x}) uv \, \mathrm{d}\mathbf{s} = \int_\Gamma fv \, \mathrm{d}\mathbf{s} \qquad \forall v \in V, \tag{2}$$

with

$$V = \begin{cases} \{v \in H^1(\Gamma) \mid \int_\Gamma v \, \mathrm{d}\mathbf{s} = 0\} & \text{if } c \equiv 0, \\ H^1(\Gamma) & \text{otherwise.} \end{cases} \tag{3}$$

Let $\{\mathcal{T}_h\}_{h>0}$ be a family of tetrahedral triangulations of the domain Ω. These triangulations are assumed to be regular, consistent and stable. We assume that for each $\mathcal{T}_h$ a polygonal approximation of Γ, denoted by Γ_h, is given: Γ_h is a $C^{0,1}$ surface without boundary and Γ_h can be partitioned in planar triangular segments. It is important to note that Γ_h is not a "triangulation of Γ" in the usual sense (an $O(h^2)$ approximation of Γ, consisting of regular triangles). Instead, we (only) assume that Γ_h is consistent with the outer triangulation $\mathcal{T}_h$ in the following sense. For any tetrahedron $S_T \in \mathcal{T}_h$ such that $\mathrm{meas}_2(S_T \cap \Gamma_h) > 0$ define $T = S_T \cap \Gamma_h$. We assume that every $T \in \Gamma_h$ is a *planar* segment and thus it is either a triangle or a quadrilateral. Each quadrilateral segment can be divided into two triangles, so we may assume that every T is a triangle. An illustration of such a triangulation is given in Figure 1. The results shown in this figure are obtained by representing a sphere Γ implicitly by its signed distance function, constructing the piecewise linear nodal interpolation of this distance function on a uniform tetrahedral triangulation $\mathcal{T}_h$ of Ω and then constructing the zero level of this interpolant.

Let $\mathcal{F}_h$ be the set of all triangular segments T, then Γ_h can be decomposed as

$$\Gamma_h = \bigcup_{T \in \mathcal{F}_h} T.$$

Note that the triangulation $\mathcal{F}_h$ is *not* necessarily regular, i.e. elements from T may have very small internal angles and the size of neighboring triangles can vary strongly, cf. Figure 1. If Γ is represented implicitly as the zero level of a level set function φ (e.g., the signed distance

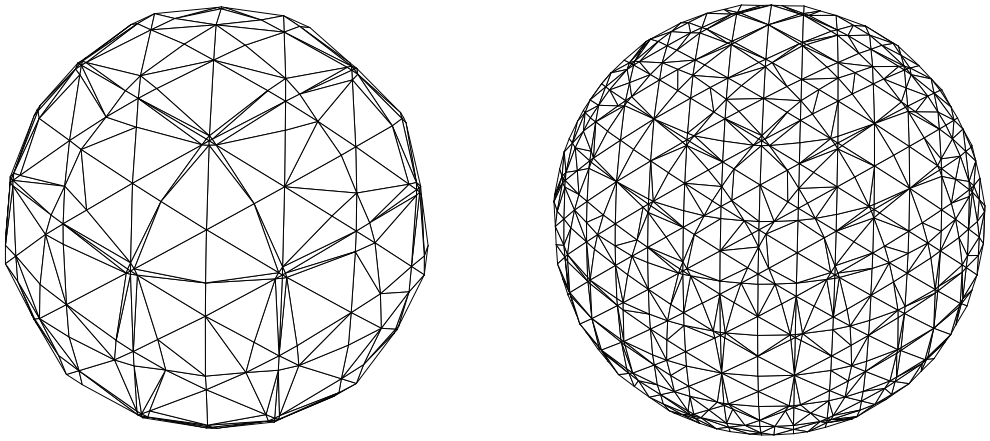

Figure 1: Approximate interface Γ_h for an example with a sphere, resulting from a coarse tetrahedral triangulation (left) and after one refinement (right).

function), then the discrete surface Γ_h can be obtained as the zero level of a piecewise linear finite element approximation to φ.

The surface finite element space is *the space of traces on Γ_h of all piecewise linear continuous functions with respect to the outer triangulation $\mathcal{T}_h$*. This can be formally defined as follows. First consider the outer space

$$V_h := \{v_h \in C(\Omega) \mid v|_S \in P_1 \ \forall\, S \in \mathcal{T}_h\}, \tag{4}$$

where P_1 is the space of polynomials of degree one. V_h induces the following space on Γ_h:

$$V_h^\Gamma := \{\psi_h \in H^1(\Gamma_h) \mid \exists\, v_h|_{S_h} \in V_h \text{ s.t. } \psi_h = v_h|_{\Gamma_h}\}. \tag{5}$$

When $c \equiv 0$, we assume that any function v_h from V_h^Γ satisfies $\int_{\Gamma_h} v_h \mathrm{d}\mathbf{s} = 0$. Given the surface finite element space V_h^Γ, the finite element discretization of (2) is as follows: Find $u_h \in V_h^\Gamma$ such that

$$\int_{\Gamma_h} \nabla_{\Gamma_h} u_h \cdot \nabla_{\Gamma_h} v_h \mathrm{d}\mathbf{s} + \int_{\Gamma_h} c^e(\mathbf{x}) u_h v_h \mathrm{d}\mathbf{s} = \int_{\Gamma_h} f^e v_h \mathrm{d}\mathbf{s} \qquad \forall\, v_h \in V_h^\Gamma. \tag{6}$$

Here c^e, f^e are suitable extensions of c and f from Γ to Γ_h, for example, by taking constant values along normals to Γ.

For the finite element method (6) the following optimal error bounds are derived in [12]:

$$\|u^e - u_h\|_{H^1(\Gamma_h)} \leq Ch\|u\|_{H^2(\Gamma)}, \qquad \|u^e - u_h\|_{L^2(\Gamma_h)} \leq Ch^2\|u\|_{H^2(\Gamma)}. \tag{7}$$

Here h is the characteristic mesh size of the outer triangulation $\mathcal{T}_h$. The result in (7) does *not* require any shape regularity of the surface triangulation $\mathcal{F}_h$.

It is clear that the elements of V_h^Γ depend only on the nodal values of outer finite element functions in the strip ω_h containing Γ_h:

$$\omega_h := \bigcup_{T \in \mathcal{F}_h} S_T.$$

Therefore, it is natural to represent the solution of (6) as a linear combination of the traces of outer nodal functions on Γ_h:

$$u_h = \sum_{i=1}^{N} u_i \phi_i|_{\Gamma_h}, \tag{8}$$

where $\{\phi_i\}$ are the nodal basis functions from V_h. In (8) only the basis functions corresponding to nodes from ω_h are used. In general, the set $\phi_i|_{\Gamma_h},\ 1 \le i \le N$, is *not* a basis, but only a generating system of the space V_h^Γ. With the representation in (8) one obtains a linear system for the coefficients u_i, $1 \le i \le N$:

$$(\mathbf{A} + \mathbf{M}_c)\mathbf{u} = \mathbf{f}, \tag{9}$$

with $\mathbf{A} = (a_{ij})_{1\le i,j\le N}$, $\mathbf{M}_c = (m_{i,j})_{1\le i,j\le N}$ and $\mathbf{f} = (f_i)_{1\le i\le N}$ given by

$$a_{ij} = \int_{\Gamma_h} \nabla_{\Gamma_h}\phi_i \cdot \nabla_{\Gamma_h}\phi_j \mathrm{d}\mathbf{s}, \quad m_{ij} = \int_{\Gamma_h} c^e(\mathbf{x})\phi_i\phi_j \mathrm{d}\mathbf{s}, \ \ f_i = \int_{\Gamma_h} f^e\phi_i \mathrm{d}\mathbf{s}. \ \ i,j = 1,\dots,N.$$

Properties of the matrices $\mathbf{A}$ and $\mathbf{M}_c$ for $c = 1$ were studied in [11]. In particular, it was shown that the diagonally scaled mass and stiffness matrices have (effective) condition numbers that scale like $\mathcal{O}(h^{-2})$, where h is the characteristic mesh size for the outer triangulation $\mathcal{T}_h$.

To solve a parabolic equation on a stationary surface, one can apply a method of lines, i.e., combine the finite element method described above with a standard finite difference discretization in time. As an example, consider the heat equation on the surface:

$$u_t - \Delta_\Gamma u = f \quad \text{on } \Gamma,$$

with initial condition $u|_{t=0} = u_0$. The application of the finite element method results in an ODE system of the form

$$\mathbf{M}_1\mathbf{u}_t + \mathbf{A}\mathbf{u} = \mathbf{f}, \tag{10}$$

which can be integrated in time numerically. In our experiments below we apply the Crank-Nicolson method:

$$\mathbf{M}_1\frac{\mathbf{u}^{n+1} - \mathbf{u}^n}{\delta t} + \frac{1}{2}\mathbf{A}(\mathbf{u}^{n+1} + \mathbf{u}^n) = \frac{1}{2}(\mathbf{f}^{n+1} + \mathbf{f}^n). \tag{11}$$

2.1 Results of numerical experiments

Two numerical examples illustrate the performance of the surface finite element method.

Example 1 The Laplace-Beltrami equation (1) is solved on the unit sphere Γ with

$$f(\mathbf{x}) = 12x_1x_2x_3.$$

By direct compuation, one checks that

$$u(\mathbf{x}) = x_1x_2x_3$$

is the solution of (1) for $c \equiv 0$.

We consider a sequence of uniform tetrahedral triangulations of $\Omega = (-2,2)^3$. The discrete surface Γ_h is the zero level of the nodal interpolant of the signed distance function to Γ, cf. Figure 1. The dimensions of the resulting surface FE spaces V_h^Γ are $N = 100$, 448, 1864, 7552, 30412. The accuracy of the method is monitored by computing the L^2 and H^1 surface errors, i.e. $err_{L2} = \|u^e - u_h\|_{L^2(\Gamma_h)}$ and $err_{H1} = \|u^e - u_h\|_{H^1(\Gamma_h)}$. The convergence plots in the log-log scale are shown in Figure 2. The results illustrate the optimal order of convergence, as was predicted by the results in (7).

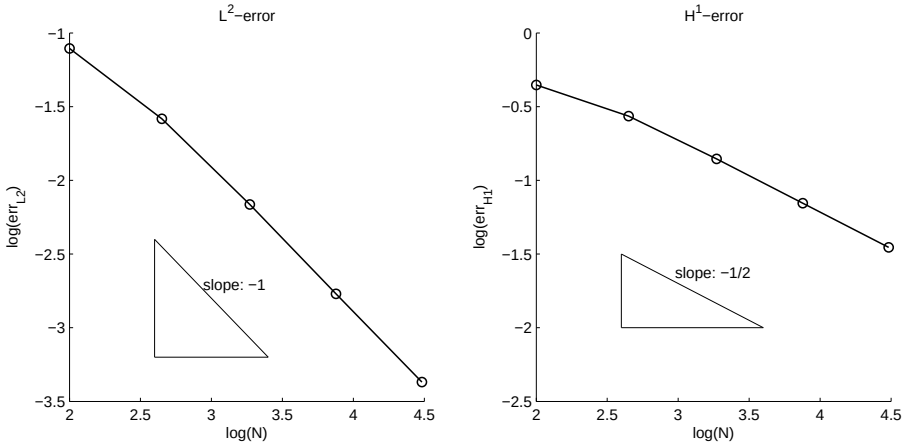

Figure 2: The L^2 and H^1 surface FE errors for Example 1.

Example 2 We consider the time-dependent surface heat equation (2) on the torus

$$\Gamma = \{(x_1, x_2, x_3) \mid (\sqrt{x_1^2 + x_2^2} - 1)^2 + x_3^2 = \frac{1}{16}\}. \tag{12}$$

We set

$$f = 100\chi_D,$$

with $D = \{\mathbf{x} \mid |\mathbf{x} - (0, 1.25, 0)| < 0.2\}$. This example models the heat diffusion over Γ, if the area D of the torus is heated with a constant heat generation rate.

We use a tetrahedral triangulation of the domain $\Omega = (-2, 2)^3$, which contains the torus. The resulting trace space V_h^Γ has $N = 5638$ degrees of freedom. For the time step in the method (11) we take $\delta t = 0.05$. The numerically computed solutions for $t = 0, 0.5, 1.5, 2.5$ are shown in Figure 3. One can clearly observe the heat diffusion on the torus.

3 SUPG STABLIZATION FOR ADVECTION-DOMINATED PROBLEMS

Let $\mathbf{w} : \Omega \to \mathbb{R}^3$ be a given divergence-free ($\operatorname{div} \mathbf{w} = 0$) velocity field in Ω. If the surface Γ evolves with a normal velocity $\mathbf{w} \cdot \mathbf{n}_\Gamma$, then the conservation of a scalar quantity u with a diffusive flux on $\Gamma(t)$ leads to the surface PDE:

$$\dot{u} + (\operatorname{div}_\Gamma \mathbf{w})u - \varepsilon \Delta_\Gamma u = 0 \qquad \text{on } \Gamma(t), \tag{13}$$

where $\dot{u}$ denotes the advective material derivative and $\varepsilon > 0$ is the diffusion coefficient. In [5] the problem (13), combined with an initial condition for u, is shown to be well-posed in a suitable weak sense.

We study the discretization of this PDE on a *steady* surface. Hence, we assume $\mathbf{w} \cdot \mathbf{n}_\Gamma = 0$, i.e. the advection velocity $\mathbf{w}$ is everywhere *tangential* to the stationary surface. The assumptions $\mathbf{w} \cdot \mathbf{n}_\Gamma = 0$ and $\operatorname{div} \mathbf{w} = 0$ imply $\operatorname{div}_\Gamma \mathbf{w} = 0$, and the surface advection-diffusion equation takes the form:

$$u_t + \mathbf{w} \cdot \nabla_\Gamma u - \varepsilon \Delta_\Gamma u = 0 \qquad \text{on } \Gamma. \tag{14}$$

We are interested in a finite element method for the advection-dominated case, i.e., $0 < \varepsilon \ll \|\mathbf{w}\|_{L^\infty(\Gamma)} |\Gamma|^{\frac{1}{2}}$.

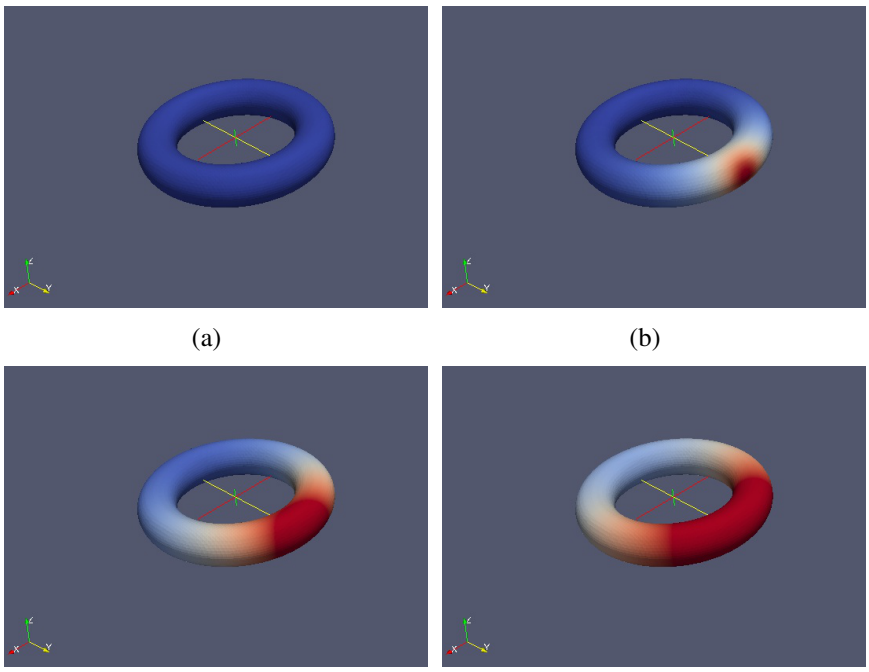

(a) (b)

(c) (d)

Figure 3: The solutions of Example 2 for $t = 0, 0.5, 1.5, 2.5$.

We first treat the stationary problem:

$$-\varepsilon\Delta_\Gamma u + \mathbf{w}\cdot\nabla_\Gamma u + c(\mathbf{x})u = f \qquad \text{on } \Gamma, \tag{15}$$

with $c(\mathbf{x}) \geq 0$ and f a given source term.

We consider a stabilized formulation of SUPG type. For this we introduce the bilinear form and the functional

$$\begin{aligned} a_h(u,v) :=& \varepsilon \int_{\Gamma_h} \nabla_{\Gamma_h} u \cdot \nabla_{\Gamma_h} v \,\mathrm{d}\mathbf{s} + \int_{\Gamma_h} c^e uv \,\mathrm{d}\mathbf{s} \\ &+ \frac{1}{2}\left[\int_{\Gamma_h} (\mathbf{w}^e\cdot\nabla_{\Gamma_h} u)v \,\mathrm{d}\mathbf{s} - \int_{\Gamma_h} (\mathbf{w}^e\cdot\nabla_{\Gamma_h} v)u \,\mathrm{d}\mathbf{s}\right] \\ &+ \sum_{T\in\mathcal{F}_h} \delta_T \int_T (-\varepsilon\Delta_{\Gamma_h} u + \mathbf{w}^e\cdot\nabla_{\Gamma_h} u + c^e u)\mathbf{w}^e\cdot\nabla_{\Gamma_h} v \,\mathrm{d}\mathbf{s}, \\ f_h(v) :=& \int_{\Gamma_h} f^e v \,\mathrm{d}\mathbf{s} + \sum_{T\in\mathcal{F}_h} \delta_T \int_T f^e(\mathbf{w}^e\cdot\nabla_{\Gamma_h} v)\,\mathrm{d}\mathbf{s}. \end{aligned} \tag{16}$$

Let h_T be the diameter of the tetrahedron S_T from the bulk mesh, which contains T, and define the cell Peclet number $\mathsf{Pe}_T := \dfrac{h_T\|\mathbf{w}^e\|_{L^\infty(T)}}{2\varepsilon}$ and $c_T = \max_{\mathbf{x}\in T} c^e(\mathbf{x})$. The stabilization parameters δ_T are based on the cell Peclet number [13]:

$$\widetilde{\delta_T} = \begin{cases} \dfrac{\delta_0 h_T}{\|\mathbf{w}^e\|_{\infty,T}} & \text{if } \mathsf{Pe}_T > 1, \\ \dfrac{\delta_1 h_T^2}{\varepsilon} & \text{if } \mathsf{Pe}_T \leq 1, \end{cases} \quad \text{and} \quad \delta_T = \min\{\widetilde{\delta_T}, c_T^{-1}\}, \tag{17}$$

with some given positive constants $\delta_0, \delta_1 \geq 0$. The stabilized finite element method for (15) reads: Find $u_h \in V_h^\Gamma$ such that

$$a_h(u_h, v_h) = f_h(v_h) \quad \forall\, v_h \in V_h^\Gamma. \tag{18}$$

The time-dependent problem can be treated with a similar approach. The stabilized spatial discretization of (14) is as follows:

$$m(\partial_t u_h, v_h)_{\Gamma_h} + \hat{a}_h(u_h, v_h) = 0, \tag{19}$$

with

$$\begin{aligned} m(\partial_t u_h, v_h) :=& \int_{\Gamma_h} \partial_t u_h v_h \,\mathrm{d}\mathbf{s} + \sum_{T\in\mathcal{F}_h} \delta_T \int_T \partial_t u_h (\mathbf{w}^e \cdot \nabla_{\Gamma_h} v_h)\,\mathrm{d}\mathbf{s}, \\ \hat{a}_h(u, v) :=& \varepsilon \int_{\Gamma_h} \nabla_{\Gamma_h} u \cdot \nabla_{\Gamma_h} v \,\mathrm{d}\mathbf{s} + \frac{1}{2}\left[\int_{\Gamma_h} (\mathbf{w}^e \cdot \nabla_{\Gamma_h} u) v \,\mathrm{d}\mathbf{s} - \int_{\Gamma_h} (\mathbf{w}^e \cdot \nabla_{\Gamma_h} v) u \,\mathrm{d}\mathbf{s}\right] \\ &+ \sum_{T\in\mathcal{F}_h} \delta_T \int_T (-\varepsilon \Delta_{\Gamma_h} u + \mathbf{w}^e \cdot \nabla_{\Gamma_h} u)\mathbf{w}^e \cdot \nabla_{\Gamma_h} v \,\mathrm{d}\mathbf{s}. \end{aligned}$$

Note that $\hat{a}_h(\cdot,\cdot)$ is the same as $a_h(\cdot,\cdot)$ in (16) with $c \equiv 0$. The resulting system of ordinary differential equations can be discretized in time by the Crank-Nicolson along the same lines as in section 2.

An alternative to the skew-symmetric discretization of the advective terms in (16) is the use of the original form of the advective term, leading to the bilinear form

$$\begin{aligned} \tilde{a}_h(u, v) :=& \varepsilon \int_{\Gamma_h} \nabla_{\Gamma_h} u \cdot \nabla_{\Gamma_h} v \,\mathrm{d}\mathbf{s} + \int_{\Gamma_h} c^e u v \mathrm{d}\mathbf{s} + \int_{\Gamma_h} (\mathbf{w}^e \cdot \nabla_{\Gamma_h} u) v \,\mathrm{d}\mathbf{s} \\ &+ \sum_{T\in\mathcal{F}_h} \delta_T \int_T (-\varepsilon \Delta_{\Gamma_h} u + \mathbf{w}^e \cdot \nabla_{\Gamma_h} u + c^e u)\mathbf{w}^e \cdot \nabla_{\Gamma_h} v \,\mathrm{d}\mathbf{s}. \end{aligned} \tag{20}$$

The bilinear forms $a_h(\cdot,\cdot)$ and $\tilde{a}_h(\cdot,\cdot)$ define different discretizations. The relation between the two is given by the equality

$$\begin{aligned} &\int_{\Gamma_h} (\mathbf{w}^e \cdot \nabla_{\Gamma_h} u) v \,\mathrm{d}\mathbf{s} \\ &\qquad = -\int_{\Gamma_h} (\mathbf{w}^e \cdot \nabla_{\Gamma_h} v) u \,\mathrm{d}\mathbf{s} - \int_{\Gamma_h} (\mathrm{div}_{\Gamma_h}\, \mathbf{w}^e) u v \,\mathrm{d}\mathbf{s} + \sum_{E\in\mathcal{E}_h} \int_E \mathbf{w}^e \cdot [\mathbf{m}_E] u v \,\mathrm{d}\mathbf{s}, \end{aligned} \tag{21}$$

where $\mathcal{E}_h$ is the set of all edges of the surface triangulation $\mathcal{F}_h$ and $[\mathbf{m}_E] = \mathbf{m}_E^1 + \mathbf{m}_E^2$, with $\mathbf{m}_E^1$ and $\mathbf{m}_E^2$ the two unit normal vectors to E, tangential to Γ_h, from the two different sides of E. Note that the last two terms do not vanish, in general.

Concerning the analysis of this SUPG method we note the following. Using $\mathrm{div}_\Gamma\, \mathbf{w} = 0$, $\mathbf{w} \cdot \mathbf{n} = 0$ and the fact that the discrete surface Γ_h is close to Γ (distance $\mathcal{O}(h^2)$) one can derive $\|\mathrm{div}_{\Gamma_h}\, \mathbf{w}^e\|_{L^\infty(\Gamma_h)} \leq ch$ and by this the second term on the right-hand side in (21) can be controlled. The last term on the right-hand side in (21) is much more difficult to deal with. Note that this term does not occur in the plane Eulerian case. The error analysis of these methods is a subject of current research and the results will be presented in a forthcoming paper.

These results show a satisfactory error bounds only for the SUPG stabilization with the skew-symmetric variant, i.e. a bilinear form as in (16). We are not able, yet, to derive satisfactory error bounds for the method with the bilinear form as in (20). Numerical experiments indicate that using the forms $a_h(\cdot,\cdot)$ and $\tilde{a}_h(\cdot,\cdot)$ works equally well, cf. below.

Finally note that in the SUPG discretizations described above the term $\Delta_{\Gamma_h} u_h$ vanishes for linear finite elements $u_h \in V_h^\Gamma$.

3.1 Results of numerical experiments

We show results of two numerical tests, which demonstrate the performance of the stabilized method.

Example 3 The stationary problem (15) is solved on the unit sphere Γ, with

$$\mathbf{w}(\mathbf{x}) = (-x_2\sqrt{1-x_3^2}, x_1\sqrt{1-x_3^2}, 0)^T.$$

This velocity field $\mathbf{w}$ is tangential to the sphere. We set $\varepsilon = 10^{-6}$, $c \equiv 0$ and consider the solution

$$u(\mathbf{x}) = \frac{1}{\pi}\arctan\left(\frac{x_3}{\sqrt{\varepsilon}}\right).$$

Note that u has a sharp internal layer along the equator of the sphere. The corresponding right-hand side function f is given by

$$f(\mathbf{x}) = \frac{4\varepsilon^{3/2}(4+\varepsilon)x_3}{\pi(\varepsilon+4x_3^2)^2}.$$

We consider the stabilized method (18) (*stbl-fem1*), the stabilized method with the alternative bilinear form (20) (*stbl-fem2*) and the standard finite element method, i.e. $\delta_T = 0$, (*std-fem*). The dimensions of the surface finite element space in this experiment are $N = 448, 1864, 7552$. The resolution is relatively low such that the sharp layers can not be resolved on these meshes. The discretization errors outside the layer are computed: $err_{L^2} = \|u - u_h\|_{L^2(D)}$ and $err_{L^{inf}} = \|u - u_h\|_{L^\infty(D)}$, with $D = \{\mathbf{x} \in \Gamma \ : \ |x_3| > 0.3\}$. Results are shown in Figure 4. We observe an $\mathcal{O}(h)$ error behavior in the L^2-norm. In this example we consider an advection-diffusion equation without a zero order term ($c \equiv 0$). We are not aware of any literature in which this (or any other) convergence behavior follows from a theoretical error analysis.

Figure 5 shows the computed solutions with the stabilized method *stbl-fem1* and the usual Galerkin method *std-fem*. Since the layer is unresolved, the standard finite element method produces globally oscillating solution. The stabilized method gives a much better approximation, although the layer is slightly smeared, as is typical for the SUPG method.

Example 4 This is an example of a time-dependent problem (14) posed on the same torus Γ as in Example 2. We set $\varepsilon = 10^{-6}$ and consider the advection field

$$\mathbf{w}(\mathbf{x}) = \frac{1}{\sqrt{x_1^2+x_2^2}}(-x_2, x_1, 0)^T.$$

The initial condition is

$$u_0(\mathbf{x}) = \frac{1}{\pi}|\mathbf{x}-\mathbf{x}_0|\arctan\left(\frac{x_3}{\sqrt{\varepsilon}}\right),$$

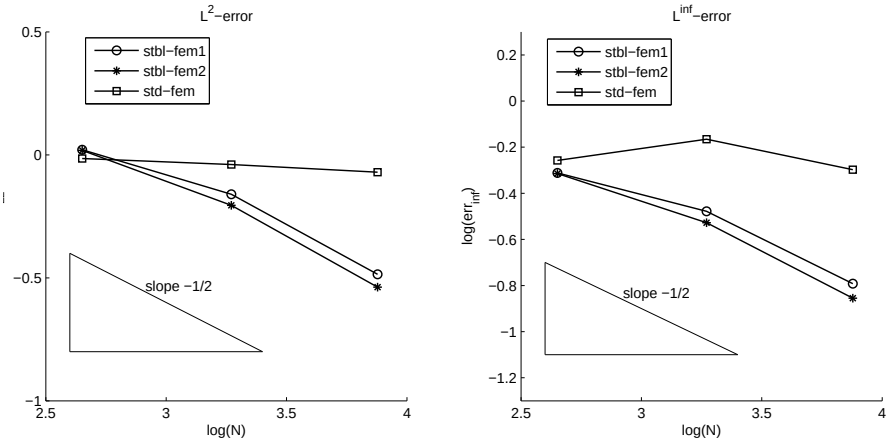

Figure 4: Convergence behavior for Example 3

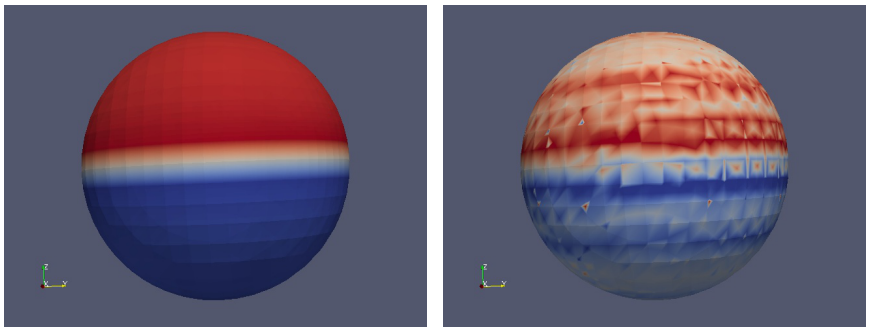

(a) (b)

Figure 5: Example 3: solutions using the stabilized method (*stbl-fem1*) and the plain Galerkin method (*std-fem*).

with $\mathbf{x}_0 = (0, -1.25, 0)^T$. The function u_0 possesses an internal layer, as shown in Figure 6(a).

For $\varepsilon = 0$ the exact solution is the transport of $u_0(\mathbf{x})$ by a rotation around the x_3 axis. Thus the inner layer remains the same for all $t > 0$. For $\varepsilon = 10^{-6}$, the exact solution is similar, unless t is large enough for dissipation to play a noticeable role. The space V_h^Γ is constructed in the same way as in the previous examples. The spatial discretization has 5638 degrees of freedom. The fully discrete problem is obtained by combining the SUPG method in (19) with a Crank-Nicolson method with time step $\delta t = 0.05$. The evolution of the solution is illustrated in Figure 6.

4 A POSTERIORI ERROR ESTIMATORS

Besides a priori error estimates, such as in (7), finite element methods are known to provide reliable tools for a posteriori error analysis, which can lead to various strategies for mesh adaptation, e.g., by local refinement. Error indicators and an adaptive version of the surface finite element method are studied in [3]. Here we outline the main result and give a few numerical examples for the Laplace-Beltrami equation (1) with $c \equiv 0$.

First, we briefly describe error indicators and an estimator. For a standard planar finite element method, a typical error indicator is the elementwise residual of a FE solution scaled by the size of the element. For the surface finite element method that we consider in this paper, the notion of the element's size is ambiguous, since the surface mesh is irregular and one may base

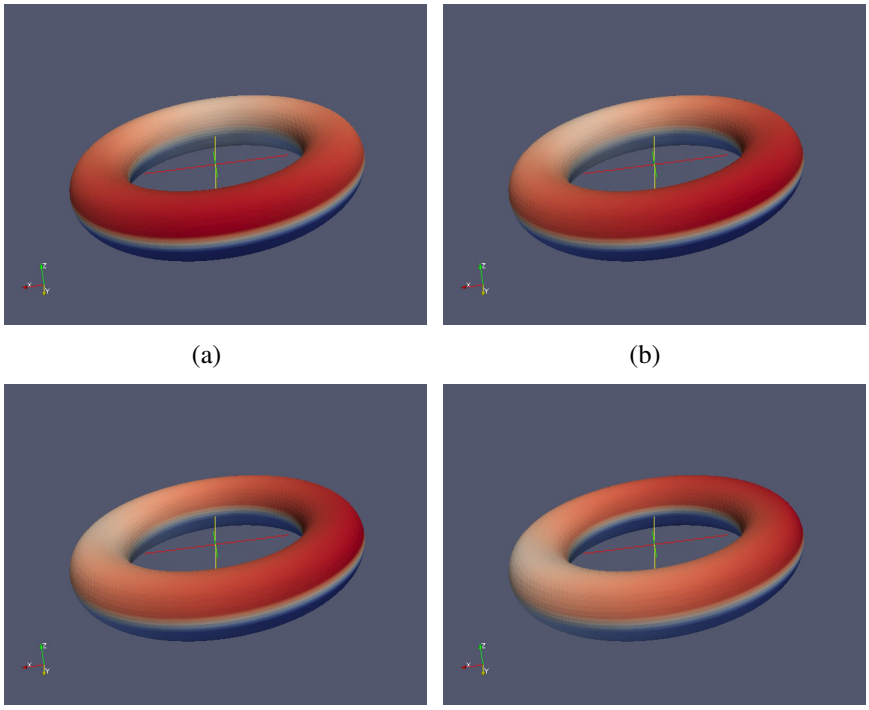

(a) (b)

(c) (d)

Figure 6: Example 4: solutions for $t = 0, 0.7, 1.4, 2.1$.

this notion for an element $T \in \mathcal{F}_h$ both on the diameter h_T of the parent (regular) tetrahedron S_T and on the area $|T|$ of the surface element. It sometimes occurs that $|T| \ll h_T^2$. To account for both possibilities, we define a family of residual-type error indicators

$$\eta_p(T) = C_p\Big(|T|^{1/2-1/p} h_T^{2/p} \|f^e + \Delta_{\Gamma_h} u_h\|_{L_2(T)} + \sum_{E\subset\partial T} |E|^{1/2-1/p} h_T^{1/p} \|[\![\nabla_{\Gamma_h} u_h]\!]\|_{L_2(E)}\Big), \qquad p \in [2,\infty]. \quad (22)$$

Here $u_h \in V_h^\Gamma$ is the finite element solution and E denotes an edge of the element T. When $p = 2$, this reduces to the expression $\eta_2(T) = C_2(h_T\|f^e+\Delta_{\Gamma_h} u_h\|_{L_2(T)}+h_T^{1/2}\|[\![\nabla_{\Gamma_h} u_h]\!]\|_{L_2(\partial T)})$ in which the diameter of the outer tetrahedron is used to measure the mesh size. At the other extreme $p = \infty$, we have instead the expression $\eta_\infty(T) = C_\infty(|T|^{1/2}\|f^e + \Delta_{\Gamma_h} u_h\|_{L_2(T)} + \sum_{E\subset\partial T} |E|^{1/2}\|[\![\nabla_{\Gamma_h} u_h]\!]\|_{L_2(E)})$ in which the properties of the surface element T are used to measure the local mesh size.

The following result (see [3]) shows the reliability up to higher order terms of a posteriori estimators obtained by summing these local indicators over all surface element. Let u and u_h be the solutions to (1) and (6), respectively. For $p \in [2,\infty)$ the following holds:

$$\|\nabla_\Gamma(u - u_h^\ell)\|_{L_2(\Gamma)} \le C\left(\sum_{T\in\mathcal{F}_h} \eta_p(T)^2\right)^{1/2} + O(h^2). \quad (23)$$

Here u_h^ℓ is the lift of the discrete surface functions to Γ. The constant C depends on the shape regularity of the outer mesh $\mathcal{T}_h$ and geometric properties of Γ such as curvature. The higher order term $O(h^2)$, where h is the characteristic mesh size of the outer mesh, corresponds to the geometric errors (resulting from the approximation of Γ by Γ_h).

The indicators $\eta_p(T)$ can be used to develop strategies for adaptive grid refinement. Numerical experiments show that such strategies lead to optimal convergence results for solutions with local singularities. In the adaptive method, we employ a "maximum" marking strategy in which all volume tetrahedra S_T from the strip ω_h with $\eta_p(T) > \frac{1}{2}\max_{T\in\mathcal{F}_h}\eta_p(T)$ are marked for further refinement.

4.1 Results of numerical experiments

Consider the Laplace-Beltrami equation (1) with $c \equiv 0$ on the unit sphere. The solution and the source term in spherical coordinates are given by

$$u = \sin^\lambda\theta\sin\phi, \qquad f = (\lambda^2+\lambda)\sin^\lambda\theta\sin\phi + (1-\lambda^2)\sin^{\lambda-2}\theta\sin\phi. \tag{24}$$

One verifies that

$$\nabla_\Gamma u = \sin^{\lambda-1}\theta\left(\frac{1}{2}\sin 2\phi(\lambda\cos^2\theta-1),\ \sin^2\phi(\lambda\cos^2\theta-1)+1,\ -\frac{1}{2}\lambda\sin 2\theta\sin\phi\right)^T$$

holds. Hence, for $\lambda < 1$ the solution u is singular at the north and south poles of the sphere so that $u \in H^1(\Gamma)$, but $u \notin H^2(\Gamma)$.

We discretize this problem in V_h^Γ using an adaptive method with local refinement based on the "maximum" marking strategy. For several values of λ the decrease of the error in H^1 and L^2 norms versus the number of d.o.f. is shown in Figure 7. The results suggest that the error estimator $\left(\sum_{T\in\mathcal{F}_h}\eta_p(T)^2\right)^{1/2}$ is both reliable and efficient and the performance depends only mildly on the value of the parameter p.

In Figure 8 we illustrate the interface triangulations obtained in the adaptive method. The results are for the parameter values $\lambda = 0.6$ and $p = 2$. In the left picture we have approximately 10^3 degrees of freedom in the finite element space V_h^Γ. The right picture shows the triangulation around a pole, with a zoom-in factor 20 and a space V_h^Γ with approximately 10^4 degrees of freedom.

5 CONCLUSIONS

We presented an overview of a special finite element method for the discretization of elliptic and parabolic partial differential equations on *stationary* surfaces. The method uses a polygonal surface approximation that is consistent with an outer tetrahedral triangulation of a domain Ω that contains the surface. Such a surface approximation can be obtained in a natural way in a level set setting. The surface finite element space is defined as the trace of a standard finite element space on the outer tetrahedral triangulation. It has been proved that for diffusion dominated problems the method has optimal order discretization accuracy. This is illustrated by results of numerical experiments. For the diffusion dominated case a residual-type error indicator has been developed and analyzed. This method is outlined and its behavior illustrated by numerical experiments. We introduce SUPG type stabilized variants of the method for advection-dominated problems. These have not been studied before. The performance of these methods is illustrated by results of numerical experiments. Important topics for current and future research are the theoretical analysis of the SUPG methods and the extension of these approaches to problems with partial differential equations on *evolving* surfaces.

Acknowledgments. This work has been supported in part by the DFG the through grant RE1461/4-1 and the Russian Foundation for the Basic Research through grants 12-01-91330, 12-01-00283. We also thank J. Grande for helping us with the implementation of the methods.

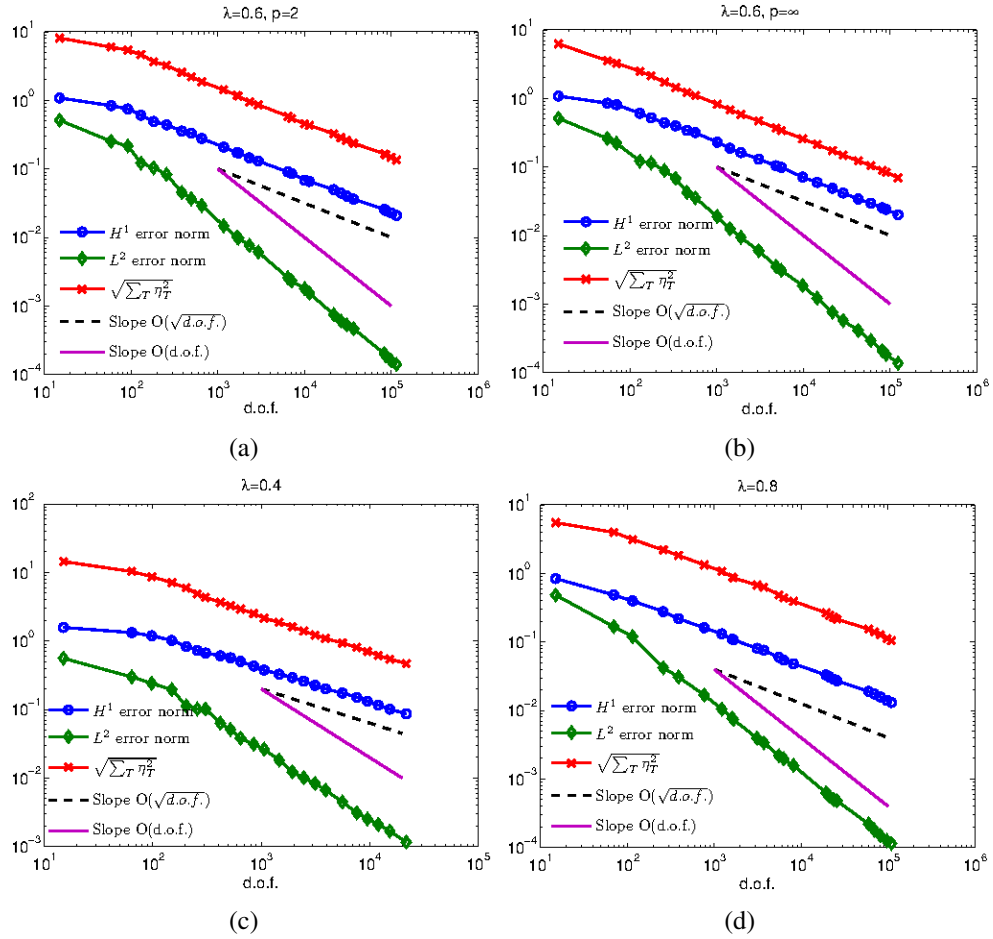

Figure 7: Decrease of the error in H^1 and L^2 norms for different values of λ. The values of the error estimator $\left(\sum_{T\in\mathcal{F}_h} \eta_p(T)^2\right)^{1/2}$ are shown. The parameter p equals 2 for figures (a),(c) and (d), while for figure (b) $p=\infty$.

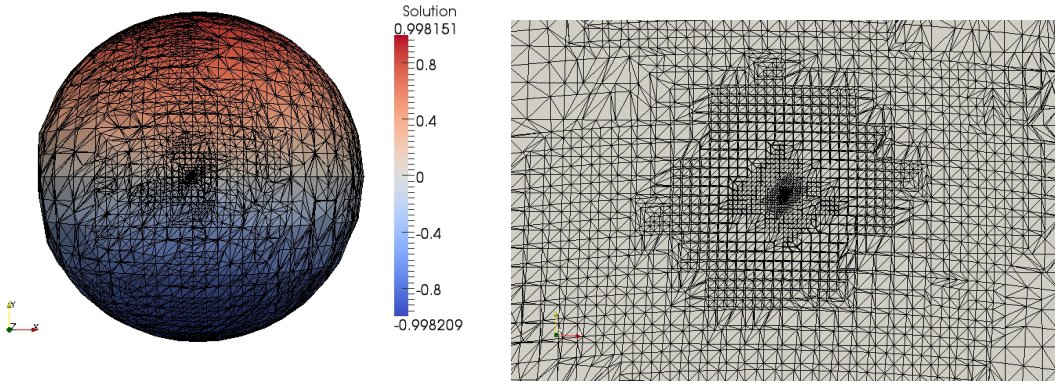

Figure 8: Interfacial triangulation Γ_h obtained with adaptive method (left) and zoom in at the pole with the factor 20 (right).

REFERENCES

[1] K. Deckelnick, G. Dziuk, C. Elliott, and C.-J. Heine. An h-narrow band finite element method for elliptic equations on implicit surfaces. *IMA Journal of Numerical Analysis*,

30:351–376, 2010.

[2] A. Demlow and G. Dziuk. An adaptive finite element method for the Laplace-Beltrami operator on implicitly defined surfaces. *SIAM J. Numer. Anal.*, 45:421–442, 2007.

[3] A. Demlow and M.A. Olshanskii. An adaptive surface finite element method based on volume meshes. *SIAM J. Numer. Anal.*, to appear.

[4] G. Dziuk. Finite elements for the Beltrami operator on arbitrary surfaces. In S. Hildebrandt and R. Leis, editors, *Partial differential equations and calculus of variations*, volume 1357 of *Lecture Notes in Mathematics*, pages 142–155. Springer, 1988.

[5] G. Dziuk and C. Elliott. Finite elements on evolving surfaces. *IMA J. Numer. Anal.*, 27:262–292, 2007.

[6] G. Dziuk and C. Elliott. Surface finite elements for parabolic equations. *J. Comp. Math.*, 25:385–407, 2007.

[7] G. Dziuk and C. Elliott. Eulerian finite element method for parabolic PDEs on implicit surfaces. *Interfaces and Free Boundaries*, 10:119–138, 2008.

[8] G. Dziuk and C. Elliott. An Eulerian level set method for partial differential equations on evolving surfaces. *Comput. Vis. Sci.*, 13:17–28, 2008.

[9] G. Dziuk and C. Elliott. L^2-estimates for the evolving surface finite element method. *SIAM J. Numer. Anal.*, 2011. to appear.

[10] S. Gross and A. Reusken. *Numerical Methods for Two-phase Incompressible Flows*, volume 40 of *Springer Series in Computational Mathematics*. Springer, Heidelberg, 2011.

[11] M. Olshanskii and A. Reusken. A finite element method for surface PDEs: matrix properties. *Numer. Math.*, 114:491–520, 2009.

[12] M. Olshanskii, A. Reusken, and J. Grande. An Eulerian finite element method for elliptic equations on moving surfaces. *SIAM J. Numer. Anal.*, 47:3339–3358, 2009.

[13] H.-G. Roos, M. Stynes, and L. Tobiska. *Numerical Methods for Singularly Perturbed Differential Equations — Convection-Diffusion and Flow Problems*, volume 24 of *Springer Series in Computational Mathematics*. Springer-Verlag, Berlin, second edition, 2008.